ABOUT SOME UNCERTAINTIES IN THE PHYSICAL AND NUMERICAL MODELING OF WAVE OVERTOPPING OVER COASTAL STRUCTURES

Romano A[1], Williams H E[2], Bellotti G[1], Briganti R[2], Dodd N[2], Franco L[1]

This paper presents an experimental and numerical study aimed at gaining insight on the variability in the wave overtopping discharge on different types of coastal structures caused by different random starting phases of incident wave sequences sharing the same energy density spectrum. The experiments on a simple rubble mound breakwater have been carried out in the wave flume of the Roma Tre University (Rome, Italy). More than 150 small scale laboratory tests were carried out to simulate spectra producing different levels of overtopping. The numerical simulations, aimed at studying the wave overtopping on a simple impermeable smooth dike, have been carried out at the University of Nottingham (Nottingham, UK). More than 4000 simulations have been performed in order to provide a statistically robust dataset. For both the physical model tests and the numerical simulations the seeding of the random number generator used for the starting phases distribution was changed a number of times for each repetition of the same wave condition. The study allowed to quantify how the variability in the wave overtopping grows as the dimensionless freeboard increases and as the number of overtopping waves decreases.

Keywords: Coastal structures; wave overtopping; laboratory experiments; numerical models

INTRODUCTION

The estimate of the wave overtopping is a crucial point in the design of coastal defences (e.g. dikes, rubble mound breakwaters, caissons, etc.). Predicting the overtopping discharge is essential to ensure the safe usability of the coastal structures and to protect the activities behind the structures themselves.

Wave overtopping has been widely studied in the past, by using mainly laboratory experiments as well as numerical tools and field measurements (e.g. CLASH project). Several empirical formulae are available to quantify the overtopping flow rates, including correction factors to take into account scale and model effects (e.g. van der Meer and Janssen, 1995; Briganti et al., 2005; Pullen et al., 2007; Franco et al., 2009; Geeraerts et al., 2009; van der Meer and Bruce, 2013). Most of these formulae estimate the mean overtopping discharge q by using as input the geometrical properties of the coastal structures (e.g. the freeboard R_c, the slope of the structure, the lenght of the berm, etc.) and the spectral wave parameters (e.g. the significant wave height H_s, the peak period T_p, etc.). As far as the wave parameters are concerned, it is worth to cite that no direct measurements of the free surface elevation are commonly available for design purposes; it implies that a synthetic sea state, described by a parametric wave spectrum, has to be used. It is important to highlight that given a synthetic energy density spectrum (e.g. JONSWAP, Pierson-Moskovitz, etc.), a theoretically infinite number of free surface elevation time series can be reconstructed from this by varying the distribution of the random starting phases (Tuah and Hudspeth, 1982). Thus, it can be supposed that the variability in the free surface elevation time series (i.e. wave sequencing, groupiness factor, maximum wave height, etc.) can affect the overtopping discharge.

First evidences on this aspect have been pointed out by Pearson et al. (2001), that performed experiments on a vertical seawall to assess the repeatability, the variability and the uncertainties in the overtopping processes. The experiments described by Pearson et al. (2001) have been performed by varying both the length of the reproduced sea state and the distribution of the random starting phases (i.e. seeding number) of each repeated wave condition. They pointed out that a variability in the overtopping mean discharge, due to both the length of the sea state and the different starting phases, can be observed. The influence of the test duration on the overtopping variability has also been investigated by Romano et al. (2014) that, by performing a sensitivity analysis carried out on the partial overtopping time series, have pointed out that shorter time series (e.g. 500 waves) can be used for overtopping tests obtaining the same order of accuracy with respect to the longer ones (e.g. the recommended 1000 waves).

The uncertainties in the overtopping prediction have been also treated in the work of McCabe et al. (2013), who pointed out that this variability can be observed both in numerical and experimental tests. More recently, Williams et al. (2014) studied numerically, on a smooth dike (seaward slope 1/2.55), the variability of the overtopping parameters given by the free surface time series of waves. By validating the numerical model against laboratory experiments, Williams et al. (2014) defined a methodology for the quantification

[1]Roma Tre University, Engineering Department, Via Vito Volterra, 62, Rome, 00146, Italy

[2]University of Nottingham, Infrastructure, Geomatics and Architecture Division, Faculty of Engineering, Nottingham, NG7 2RD, UK

of this uncertainty in the estimation of individual overtopping volumes and mean discharges.
Therefore, overtopping parameters exhibit a variability due to the reconstruction of the offshore boundary time series (i.e. free surface elevation time series). It was found that the lower the overtopping percentage, the higher the variability. The variability is also larger for the overtopping volumes. This is important as most of coastal structures are usually designed to allow a low percentage of overtopping waves. As for laboratory experiments, McCabe et al. (2013) pointed out that the repeatability of two nominally identical flume experiments is only within 25 %. Different distributions of random phases between spectral components can induce much larger discrepancies between tests with identical nominal sea state parameters.
This paper aims at studying by means of laboratory experiments and numerical simulations the uncertainties in estimating the overtopping rates caused by different distributions of random starting phases of the spectral components that are used to reconstruct the free surface elevation time series to be reproduced. A large number of laboratory small scale model tests on a simple rubble mound breakwater (Froude law scale 1:20) and numerical simulations on a simple impermeable smooth dike have been carried out by varying the seeding number (i.e. the distribution of the random starting phases) for each wave condition.
The paper is structured as follows: after this introduction a description of the experimental and the numerical setup is given, then the overtopping data are shown and discussed. Finally, the concluding remarks close the paper.

LABORATORY EXPERIMENTS

The laboratory experiments have been carried out in the wave flume at the hydraulic laboratory of the Roma Tre University. The flume is $9.00\,m$ long, $0.27\,m$ wide and $0.50\,m$ high. It is made of plexiglass panels ($0.02\,m$ thick) sustained by a steel frame. At one end a piston wave-maker is installed; it consists of a vertical steel plate driven by a remotely controlled electric motor. The effective stroke of the piston wave-maker is $1.00\,m$. The system is able to generate, using a Matlab code developed in house, both regular and irregular waves.
The tests were carried out on a simple rubble mound breakwater with a seaward armour slope of 1:2.5 (see Figure 1). The structure had an impermeable core of river sand (nominal diameter, $D_{n50} = 0.5\,mm$). The armour consisted of two layers of randomly placed natural stones (density, $\rho_s = 2.6\,t/m^3$, $D_{n50} = 50\,mm$). Furthermore a parapet wall of plastic material was placed on the top of the core behind the landward armour units.
The overtopping volumes were collected using a chute fixed to the crest of the parapet wall. At the end of the chute a hole, placed on the sloping bottom of the chute itself, allowed the water to flow into a rubber pipe ($1.0\,m$ long) that collected the overtopped water into a tank placed outside the wave flume. A load cell was then connected to the overtopping tank in order to measure the volume in time. The sketch of the experimental set-up is showed in the upper panel of Figure 1.
Four resistive wave gauges were placed along the flume for the measurement of the free surface. The positions of the wave gauges, measured with respect to the rest position of the wave paddle, are $x_{S1} = 1.85\,m$, $x_{S2} = 2.10\,m$, $x_{S3} = 7.25\,m$ and $x_{S4} = 7.5\,m$ respectively. The incident wave conditions (H_{m0i}) in the flume were computed with the Goda and Suzuki (1976) method using the $S1$ and $S2$ gauges away from the structure and the $S3$ and $S4$ at the toe. Very similar results were obtained by the two couples given the short length of the flume.

R_c (m)	H_{m0} (m)	$\overline{H_{m0i}}$ (m)	T_p (s)	R^*	Repetitions
0.11	0.105	0.101	1.62	1.047	4
0.11	0.097	0.095	1.56	1.134	4
0.11	0.089	0.086	1.49	1.236	20
0.11	0.081	0.079	1.42	1.358	25
0.11	0.077	0.075	1.39	1.428	25
0.11	0.073	0.071	1.35	1.506	25
0.11	0.065	0.062	1.27	1.692	25
0.11	0.056	0.053	1.19	1.964	25

Table 1: Experimental conditions.

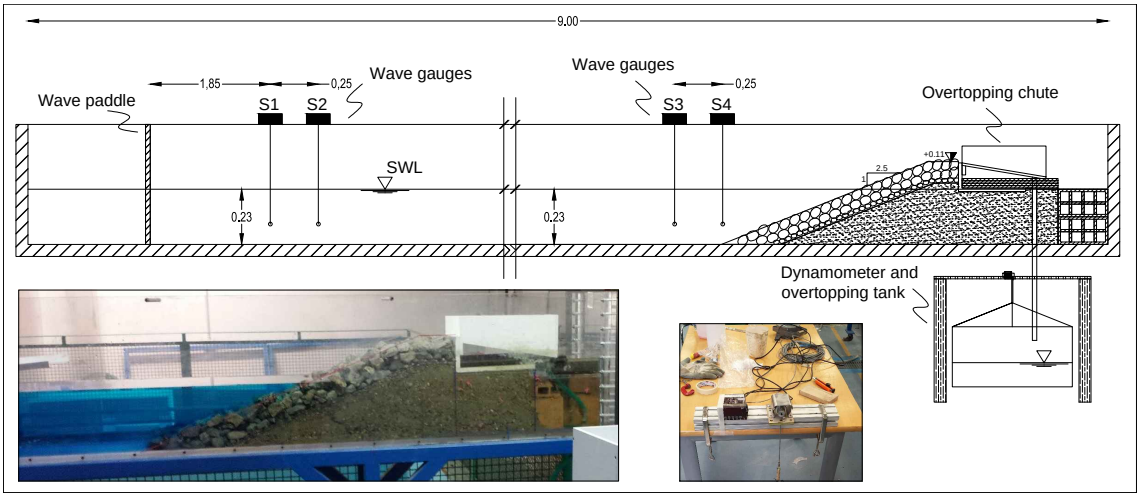

Figure 1: Upper panels: sketch of the experimental set-up. Lower panel: pictures of the wave flume and of the model structure.

The still water depth was kept constant throughout the experimental campaign ($h = 0.23\,m$), thus the freeboard R_c had a constant value of 0.11 m. Eight wave conditions defined by the significant target wave height H_{m0} and by the peak period T_p at the paddle, and in turn eight values of the dimensionless freeboard $R^* = R_c/H_{m0}$, were tested and repeated several times (see Table 1 for the target values). In each of these repetitions the distribution of the random starting phases was changed, thus the generated free surface elevation time series changed each time. Note that the average values of the incident wave height ($\overline{H_{m0i}}$) obtained for each combination of R_c and H_{m0} are reported in the third column of the Table 1.
In order to easily perform a large number of experiments, a batch procedure was implemented in the wave flume. The first step of the procedure consisted in defining a JONSWAP wave energy density spectrum with peak enhancement factor $\gamma = 3.3$ and with the target H_{m0} and T_p. Then, a free surface elevation time series containing approximately 1000 waves was created by using a distribution of starting phases once a seed number for the random number generator was assigned. Thus, the waves were generated in the wave flume and the overtopping volumes (if any) were collected into the overtopping tank. At the end of the experiment an automatic procedure checked the water level inside the wave flume. If this did not change noticeably during the previous experiment, the procedure allowed the computer to create a new free surface elevation time series by using the same wave spectrum but with a different seeding number (i.e. different distribution of the random starting phases), and a new experiment could be performed. Otherwise, the check procedure stopped the generation of the new time series; the flume had to be manually refilled before a new experiment could be performed.

NUMERICAL SIMULATIONS

The numerical simulations were carried out at the University of Nottingham using the solver of the Non-Linear Shallow Water Equations (hereinafter NLSWE) based on a finite volume scheme using a Weighted Averaged Flux (WAF) proposed in Briganti et al. (2011). The hydrodynamics equations are:

$$\frac{\partial h}{\partial t} + \frac{\partial hU}{\partial x} = 0 \tag{1}$$

$$\frac{\partial hU}{\partial t} + \frac{\partial \left(hU^2 + \frac{1}{2}gh^2\right)}{\partial x} = -gh\frac{\partial z_B}{\partial x} - \frac{\tau_b}{\rho}. \tag{2}$$

x is the horizontal abscissa, t is time, U denotes the depth-averaged horizontal velocity and z_B is the bed level. $h = d + \eta$ where d is the still water depth and η the free surface. τ_b the bottom shear stress and ρ is the water density.

Test	T_p (s)	H_{m0} (m)	d_t (m)	R_c (m)
001	1.30	0.085	0.09	0.21
002	1.76	0.032	0.09	0.21
003	2.20	0.036	0.09	0.21
004	1.32	0.026	0.13	0.17
005	1.76	0.031	0.13	0.17
006	2.20	0.038	0.13	0.17
007	1.76	0.075	0.09	0.21
008	1.20	0.081	0.09	0.21

Table 2: Incident wave conditions measured at the structure toe from the JONSWAP spectrum random wave laboratory tests.

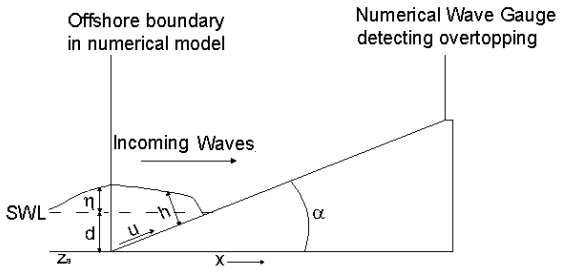

Figure 2: Numerical Model Domain

The numerical domain can be seen in Figure 2. The structure was a simple smooth sloped structure with a seaward slope of 1/2.55, with varying freeboard depending on the test conditions. In these tests, an energy density spectrum obtained from the measurement of incident time series of η during physical model tests, carried out at HR Wallingford, were used to generate a population of time series for the numerical model. Details of the wave conditions can be found in Table 2. The amplitudes of the spectral components used were obtained directly from the spectrum. An initial seed value was required for the starting phases to generate a uniform distribution between 0 and 2π across the domain. The components were then combined to produce the different times series of η. Since the incident spectrum was used, an absorbing generating boundary condition was used following the approach in Kobayashi and Wurjanto (1989) and Dodd (1998). To allow a statistically relevant comparison of the variability in the results due to these reconstructed time series, 500 tests were carried out for each wave spectra measured in the laboratory.

In order to measure the wave overtopping in the numerical model, a virtual wave gauge was located at the crest of the structure. Here, h and U were used to measure each overtopping event. The overtopping volume V_{ovt} was computed by integrating in time the discharge $Q = hU$ during the duration of the event itself.

RESULTS AND DISCUSSION

In this section the overtopping results are presented and discussed. The first part describes the variability on the wave overtopping discharge measured in the laboratory experiments, while the second part illustrates the same evidences obtained by means of the numerical simulations. It is worth to recall that the two sets of data refer to different types of structures, i.e. a rubble mound breakwater was tested in laboratory experiments while a smooth impermeable dike was reproduced in the numerical model. Nevertheless, the next sections illustrate how the overtopping variability due to the different distribution of the random starting phases of the spectral components can affect both the tested structures, regardless of the model that is used to estimate the wave overtopping flow rate.

Variability of the overtopping discharge in the laboratory experiments

The results of the tests confirmed a significant variability of the overtopping discharge among the wave sequences tested. Figure 3 shows, as an example, the overtopping volume time series measured in 25 tests with the same energy density spectrum ($H_{m0} = 0.081\,m$, $T_p = 1.42\,s$) but with different seeds for the starting phases distributions. With these conditions the total overtopped volume varied in the range $0.5 - 1.5\,l$.
The measured mean overtopping discharges are shown in Figure 4 (note that the data are represented in model scale). The left panel of Figure 4 shows the mean overtopping discharge q as a function of the dimensionless parameter R^*. In order to have a clearer visualization of the variability of the q, the data have been plotted by using the target incident H_{m0} at the paddle, instead of the measured incident conditions at the toe.

Each cluster of markers indicates a different wave condition, while each marker within it represents a different seeding for the free surface elevation time series. In the same plot also the expected value of the overtopping discharge, calculated with the EurOtop (see formula 5.8, Pullen et al., 2007), is represented with a gray line. The increase of variability with larger R^* is evident. In particular, when the dimensionless freeboard R^* is larger than 1.69, the variability of the overtopping discharge reaches one order of magnitude for the same wave condition. Sets with R^* smaller than 1.2 show a 20% variability. It is worth to note that these results are consistent with the work by Williams et al. (2014). Further similarities can be observed in the right panel of Figure 4. This shows q as a function of the overtopping probability P_{ovt}. The number of overtopping events has been estimated using a detection method similar to that shown in McCabe et al. (2013). Given the small scale of the experiment and the method used to collect the overtopping water, the computation of P_{ovt} is not accurate as small events may not be detected. However, the plot is useful to show the analogies with the findings of Williams et al. (2014). q varies of two orders of magnitude for $P_{ovt} = 0.2$ % and of less than one order of magnitude when $P_{ovt} = 5$ %. The estimated P_{ovt} is lower than 5% in all tests and the variability of P_{ovt} within the same set of tests is significant.
In order to better understand the variability in the context of engineering applications, the experimental data are plotted in dimensionless form (i.e. $q^* = \frac{q}{\sqrt{gH_{m0}^3}}$, g being the gravity acceleration) against R^* (see Figure 5). This allows a direct comparison between the present findings and the confidence levels of the formulae proposed in EurOtop (see formula 5.8, Pullen et al., 2007). Figure 5 clearly shows that the experimental confidence intervals fall well within the prediction ones. Note that the experimental variability is always one order of magnitude smaller than the prediction one, even at larger values of R^*. We refer to Romano et al. (2014) for further details.

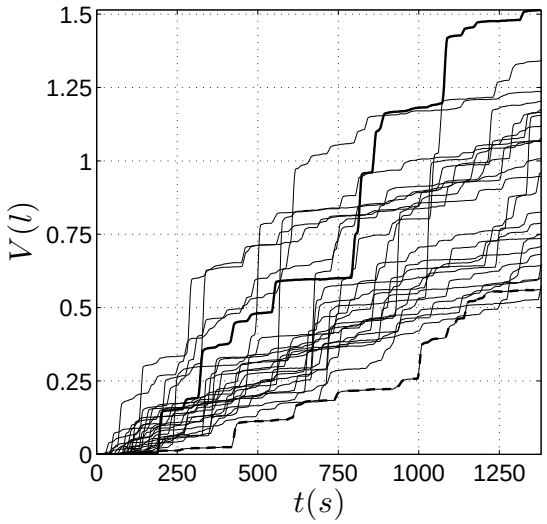

Figure 3: Overtopping volume time series obtained for 25 repetitions of the same sea state ($H_{m0} = 0.081\,m$, $T_p = 1.42\,s$) with varying the seeding number. Thick black and dashed black lines represent the maximum and the minimum final overtopping volume respectively.

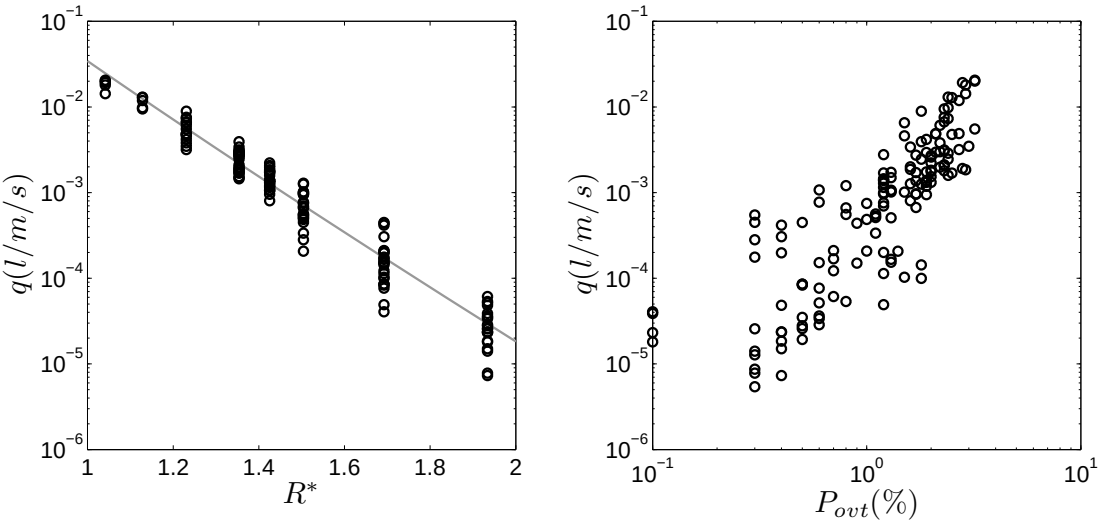

Figure 4: Left panel: mean overtopping discharge q as a function of the dimensionless parameter R^*. Black circles: experimental data; gray line indicates the expected value as from the EurOtop (see formula 5.8, Pullen et al., 2007). Right panel: mean overtopping discharge q as a function of the probability of overtopping. Note: all the data are represented in model scale.

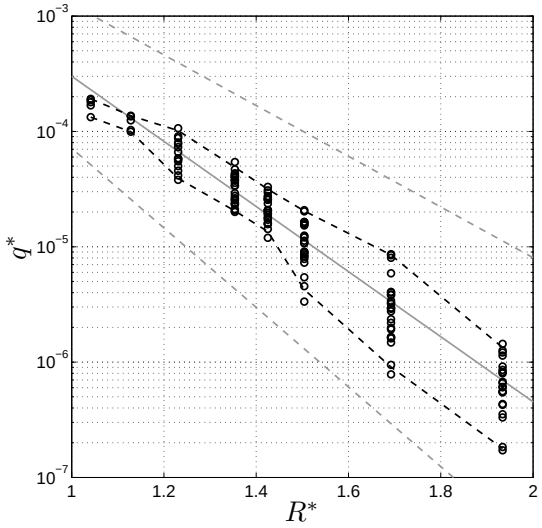

Figure 5: Dimensionless mean overtopping discharge q^* as a function of the dimensionless parameter R^*. Black markers: experimental data; dashed black lines indicate the lower and upper 5 % confidence intervals of the measurements distributions; gray line identifies the predicted dimensionless overtopping discharge; dashed gray lines represent the lower and upper 5 % confidence intervals using the EurOtop (see formula 5.8, Pullen et al., 2007).

Overtopping uncertainties in the numerical simulations

The variability of the numerical tests are examined in detail in Williams et al. (2014), here an overview of the results is included. A scatter plot of q against P_{ovt} has been produced for all of the numerical test results (see Figure 6). It can be seen on this plot that the variability in the predicted q is strictly related to the P_{ovt} in each test.

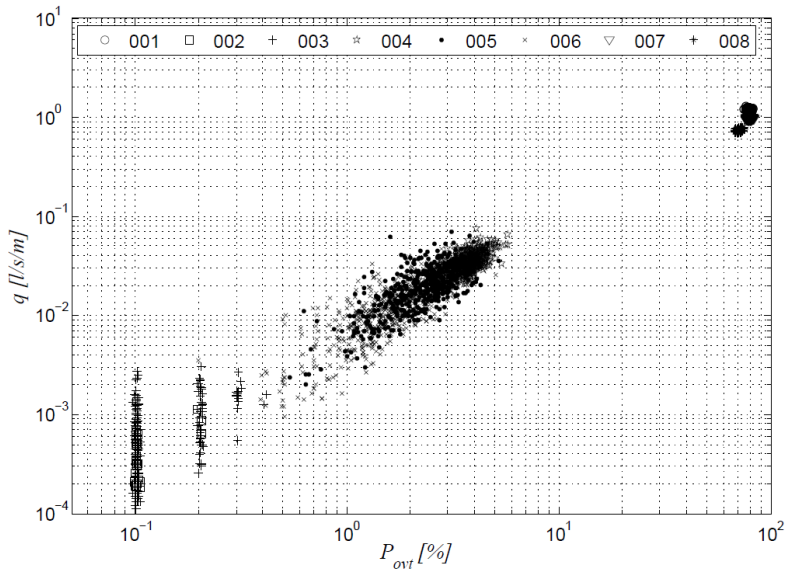

Figure 6: Logarithmic graph showing the correlation between P_{ovt} and q for the 8 numerical test conditions.

In tests 002 and 003, P_{ovt} remains lower than 1% while q varies by more than 25 times, i.e. the highest discharge is more than 25 times larger than that of the lowest discharge recorded. It should also be noted that many of the Reconstructed Offshore Boundary Conditions (ROBC) tests in this range of values experienced no overtopping in a number of the runs. These values are not reported in Figure 6 as all $q = 0$ would also have $P_{ovt} = 0$.

Tests 004, 005 and 006 continue to show large variability in terms of orders of magnitude of P_{ovt}, which varies from 0.2% to 6%. A similar magnitude of variation to the low overtopping tests is also present in the values of q. Then the tests (001, 007 and 008) with the highest values of P_{ovt} and q show very little variability in the overtopping parameters. This behaviour can be straightforwardly explained: when few waves are overtopping, the relative importance of each event is large. Conversely, with an increasing number of these events, the role of the individual waves becomes smaller.

Overall, the results from the numerical model tests show that offshore boundary conditions for NLSWE solvers derived from energy density spectra play a very important role in the simulation of overtopping at coastal structures. In particular, the higher level of uncertainty for low overtopping conditions is important in the design of coastal structures as these are usually designed to allow a low percentage of overtopping waves. It is within this region that the variability due to the seeding is larger and it is suggested that the numerical prediction of overtopping should be carried out using more than one numerical test starting from spectral offshore boundary conditions. From the figure a value of $P_{ovt} < 5\%$ should be taken as the limit value of P_{ovt} for which a sensitivity analysis is needed as this is the region where results vary more than one order of magnitude.

CONCLUSIONS

In this paper the uncertainties in the physical and numerical modelling of the wave overtopping that occurs at different types of coastal structures have been studied. The paper quantifies the variability in the overtopping parameters given by the distribution of the random starting phases in equally energetic wave sequences with varying R^*. The laboratory tests, carried out on a simple rubble mound breakwater, have shown that this variability is one order of magnitude smaller than the confidence intervals of the Pullen et al. (2007) formulae and as also shown in Williams et al. (2014), it grows with R^* up to $R^* = 1.69$, when q varies more than one order of magnitude regardless of the value of the dimensionless freeboard.

The numerical simulations, carried out on a simple impermeable smooth dike, have shown that the variability on the wave overtopping is strongly related to the overtopping probability P_{ovt}. As the percentage

of overtopping waves decreases then the uncertainty in estimating the overtopping parameters increases. In particular when $P_{ovt} < 5\%$ the results have shown a variability of more than one order of magnitude. Finally it is worth to cite that these conditions are very common in the coastal strucures design practice, given that the structures themselves are generally designed to minimize the overtopping discharge (i.e. low percentage of overtopping waves). Although more tests involving different types of structures are needed, the results obtained here suggest the possibility of revising overtopping laboratory test practice.

ACKNOWLEDGEMENTS

Riccardo Briganti and Hannah Williams were supported by the EPSRC Career Acceleration Fellowship (EP/I004505/1).

References

R. Briganti, G. Bellotti, L. Franco, J. De Rouck, and J. Geeraerts. Field measurements of wave overtopping at the rubble mound breakwater of Rome–Ostia yacht harbour. *Coastal engineering*, 52(12):1155–1174, 2005.

R. Briganti, D. Dodd, N.and Pokrajac, and O. T. Non linear shallow water modelling of bore-driven swash: Description of the bottom boundary layer. 58(6)(http://dx.doi.org/10.1016/j.coastaleng.2011.01.004): 463–477, 2011.

N. Dodd. A numerical model of wave run-up, overtopping and regeneration. 124(2):73–81, 1998.

L. Franco, J. Geeraerts, R. Briganti, M. Willems, G. Bellotti, and J. De Rouck. Prototype measurements and small-scale model tests of wave overtopping at shallow rubble-mound breakwaters: the ostia-rome yacht harbour case. *Coastal Engineering*, 56(2):154–165, 2009.

J. Geeraerts, A. Kortenhaus, J. González-Escrivá, J. De Rouck, and P. Troch. Effects of new variables on the overtopping discharge at steep rubble mound breakwaters—the Zeebrugge case. *Coastal Engineering*, 56(2):141–153, 2009.

Y. Goda and T. Suzuki. Estimation of incident and reflected waves in random wave experiments. *Coastal engineering proceedings*, 1(15), 1976.

N. Kobayashi and A. Wurjanto. Wave overtopping on coastal structures. 115(2):235–251, 1989.

M. McCabe, P. Stansby, and D. Apsley. Random wave runup and overtopping a steep sea wall: Shallow-water and boussinesq modelling with generalised breaking and wall impact algorithms validated against laboratory and field measurements. *Coastal Engineering*, 74:33–49, 2013.

J. Pearson, T. Bruce, and N. Allsop. Prediction of wave overtopping at steep seawalls–variabilities and uncertainties. In *Proceedings Waves*, volume 1, pages 1797–1808, 2001.

T. Pullen, N. Allsop, T. Bruce, A. Kortenhaus, H. Schüttrumpf, and J. Van der Meer. Wave overtopping of sea defences and related structures: assessment manual. *Environment Agency, UK*, 2007.

A. Romano, G. Bellotti, R. Briganti, and L. Franco. Uncertainties in the physical modelling of the wave overtopping over a rubble mound breakwater: the role of the seeding number and of the test duration. *Submitted to Coastal Engineering*, 2014.

H. Tuah and R. T. Hudspeth. Comparisons of numerical random sea simulations. *Journal of the Waterway Port Coastal and Ocean Division*, 108(4):569–584, 1982.

J. van der Meer and T. Bruce. New physical insights and design formulas on wave overtopping at sloping and vertical structures. *Journal of Waterway, Port, Coastal, and Ocean Engineering*, 2013.

J. W. van der Meer and J. P. F. M. Janssen. *Wave run-up and wave overtopping at dikes*. N. Kobayashi, Z. Demirbilek (Eds.), Wave Forces on Inclined and Vertical Structures, pp. 1–27 Ch. 1, 1995.

H. E. Williams, R. Briganti, and T. Pullen. The role of offshore boundary conditions in the uncertainty of numerical prediction of wave overtopping using non-linear shallow water equations. *Coastal Engineering*, 89:30–44, 2014.